



OPEN

Molecular simulation of the effect of water content on CO₂, CH₄, and N₂ adsorption characteristics of coal

Lin Hong^{1,2}, Jiaying Lin^{1,2✉}, Dameng Gao^{1,2,3}, Dan Zheng^{1,2} & Wenzhuo Wang⁴

The objective of this work was to investigate the sorption behavior of gases, namely CO₂, CH₄, and N₂, by molecules of coal sampled from Linglu mine under different water inclusion rates. To this end, the adsorption, diffusion, adsorption heat, and potential energy distribution characteristics of the gases in the coal pores at different water inclusion rates were analyzed using molecular dynamics and grand canonical ensemble Monte Carlo methods. The results showed that the adsorption relationship of the coal molecules on CO₂, CH₄, and N₂ exhibited a downtrend followed by an uptrend when the water content was increased from 0 to 3.6%. The adsorption amount of CO₂ was approximately twice as much as those of CH₄ and N₂, indicating that the competitive adsorption advantage of CO₂ compared with those of CH₄ and N₂ was unaffected by the water content. The trend in the average heat of adsorption was generally consistent with the trend in the density of coal molecules under different moisture contents. Under the same conditions, the diffusion coefficient within a coal molecule was negatively related to the water content in the system. The layer spacing of the water molecules (2.875 Å) was greater than the liquid–water layer spacing, indicating the formation of a water molecule layer at this point, which inhibited gas adsorption. This study lays a theoretical foundation for further investigating the microscopic mechanism of coal–water interaction.

Keywords Molecular dynamics, Grand canonical ensemble Monte Carlo, Radial distribution function, Diffusion, Energy distribution

The adsorption process of water molecules by coal is relatively complex and is a combined result of intermolecular electrostatic forces and hydrogen bonding^{1,2}. Several studies have reported that the adsorption of CO₂, CH₄, and N₂ by coal macromolecules decreases with the increase in the number of water molecules^{3–5}. However, there is literature confirming the role of water molecules in facilitating the adsorption of methane⁶.

In an attempt to study the sorption characteristics and thermodynamic properties of CO₂, CH₄, and N₂ on coal under different water contents, scholars at home and abroad have conducted a series of experiments^{7–9} and simulations^{10,11}. Li et al.^{12–14} simulated the sorption properties of coal on CO₂ and CH₄ at various water inclusion rates and pore sizes using the grand canonical ensemble Monte Carlo (GCMC) method and verified that the sorption of CH₄ and CO₂ by coal molecules is negatively correlated with the water inclusion rate. Zhang et al.^{15–17} analyzed the effects of the temperature and content of moisture on the isotherms and thermodynamic properties of CH₄ adsorption through simulations. Gao et al.^{18,19} verified that the greater the amount of water injection, the lower the desorption of the gas. Thus, water injection can decrease the risk of coal and gas protrusion. Wang et al.^{20,21} quantitatively characterized the effects of adsorbed water and water vapor on coal gas sorption by nuclear magnetic resonance (NMR) spectroscopy. The results showed that water vapor preferred to adsorb in the coal micropores, while liquid water filled the extensive network of pores and cracks. Xing et al.²² verified that water competes with CH₄ for specific sorption sites, resulting in a reduced CH₄ sorption capacity for shales containing water. Environmental factors, such as the pressure, temperature, and other external factors, can also vary the water distribution and endowment in shale, thus affecting the CH₄ sorption capacity of shale

¹College of Safety Science & Engineering, Liaoning Technical University, No.188 Longwan South Street, Huludao 125105, Liaoning, China. ²Key Laboratory of Mine Thermodynamic Disaster & Control of Ministry of Education, Liaoning Technical University, Huludao 125105, Liaoning, China. ³Institute of Mine Safety Technology, China Academy of Safety Science and Technology, Beijing 100012, China. ⁴Linglu Coal Mine of China Huaneng Group Co., Ltd., Beijing, China. ✉email: m13596843024@163.com

to a certain extent²³. Zhang et al.²⁴ used a combination of X-ray photoelectron spectroscopy (XPS), mercury intrusion porosimetry (MIP), and high-pressure volumetric method to quantitatively analyze the adsorption behavior of CH₄ in tectonic coals under the influence of moisture. They further verified that the sorption capacity of CH₄ decreases with an increase in the water content. Guo et al.²⁵ tested coal samples with different water contents by developing a new type of device for water injection gas adsorption. Some foreign scholars have studied the adsorption characteristics and thermodynamic analysis of coal containing different amounts of water. Chattaraj et al.²⁶ discussed the adsorption behavior of coalbed methane and showed that the adsorption process can be better explained in terms of thermodynamics and its molecular dynamics (MD). Men'shchikov et al.²⁷ studied the porous structure, phases, and chemical properties of activated carbon through experimental methods such as nitrogen adsorption, X-ray diffraction, and scanning electron microscopy. The sorption of CH₄ and the thermodynamic properties of the sorption system were analyzed. Gensterblum et al.²⁸ measured the sorption isotherms of CH₄ and CO₂ for coal samples of various coal grades at dry and moisture equilibria and investigated the variation in the sorption capacities of CH₄ and CO₂ by coals of different grades, as well as the effect of water on the sorption characteristics. Muangthong-On et al.²⁹ measured the heat of sorption/desorption of water on coal using thermogravimetric analysis and differential scanning calorimetry (TG-DSC) at temperatures exceeding 100 °C. They demonstrated that the adsorption of water vapor plays an important role in the self-heating of coal. These studies have provided a basis to study the sorption/desorption characteristics of coal on gas under different water contents.

Most studies on the effect of water addition on coal sorption/desorption characteristics have focused on macroscopic phenomena, while studies on microscopic mechanisms are fewer and less in-depth. Therefore, in this work, the adsorption/desorption characteristics and thermodynamic properties of CO₂, CH₄, and N₂ by molecules in the Linglu mine coal with different water contents were quantitatively analyzed by simulating the injection of different amounts of water molecules into the coal seam, which is crucial for the suppression of coal-gas protrusion.

Methodology

Coal model building and optimization

The adsorption of coal on gas can be categorized as a physical adsorption process^{30,31}. In response to this paper, based on the test results of coal samples from Linglu coal mine, the molecular structure model of coal (C₂₁₆H₁₆₉O₁₂N₄) was established to study the adsorption characteristics of CO₂, CH₄, and N₂ on coal with different moisture contents taken from the Linglu mine. The established 2D model was imported into the Materials Studio software, and the structure was subjected to geometric optimization, energy optimization, and simulated annealing with a minimum value of annealed energy. The simulation parameters are shown in Table 1. Table 2 presents the optimized energy parameters. Figure 1 shows the optimized molecular models of the Linglu mine coal, where 10, 20, and 30 molecules of water are added to the computational cell using the amorphous cell module. Figure 2 shows the ultracrystalline cell model of this coal constructed under different water content conditions.

Parameter settings for adsorption kinetics simulation

The adsorption laws and influencing characteristics of CO₂, CH₄, and N₂ adsorption by the molecules of the Linglu mine coal at different temperatures (273.15, 283.15, 293.15, 303.15, and 313.15 K) and water contents were analyzed based on the GCMC simulation method. A geometry optimization of the coal molecular fragments was performed using the Forcite module with the simulation parameters listed in Table 3. The MD method was then applied to analyze the diffusion and flow ability of the water molecules, and the NVT system with a constant number of molecules (*N*), constant volume (*V*), and constant temperature (*T*) was selected to run the MD simulations. The temperature was fixed using the Berendsen thermostat. In the MD operation, the simulation

Setting	Parameter
Summation method	Atom based
Truncation	Cubic spline
Spline width	1 Å
Buffer width	0.5 Å

Table 1. Optimized parameter settings for coal molecular modeling at Linglu mine.

<i>E</i> _{total} (kcal/mol)	<i>E_v</i> (kcal/mol)				<i>E_N</i> (kcal/mol)		
	<i>E_B</i>	<i>E_A</i>	<i>E_T</i>	<i>E_I</i>	<i>E_{VAN}</i>	<i>E_E</i>	<i>E_H</i>
14,452.484	5439.979	1189.461	1471.321	191.326	4028.284	5.50	− 2.320

Table 2. Energetic parameters for the optimization of the molecular structure of Linglu mine coal. *E_v* valence energy, *E_B* bond energy, *E_A* angle energy, *E_T* torsion energy, *E_I* inversion energy, *E_N* nonbond energy, *E_{VAN}* van der Waals energy, *E_E* electrostatic energy, *E_H* hydrogen bond energy.

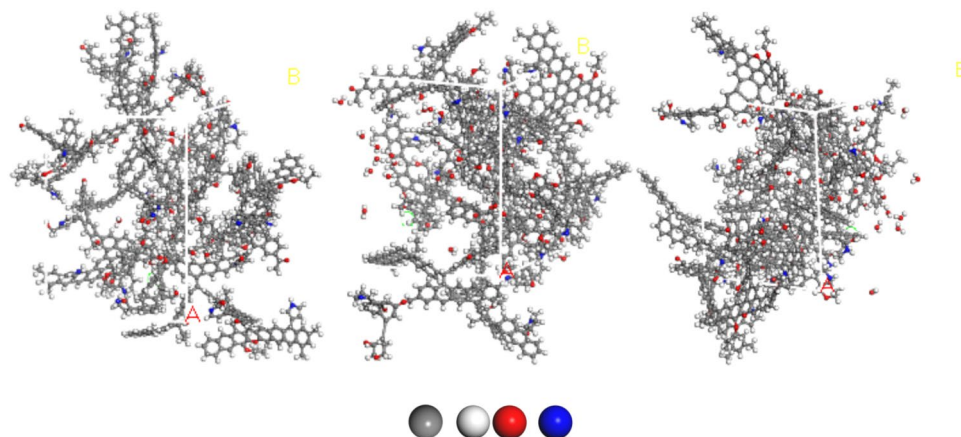


Figure 1. Pore structure model of the coal from Linglu mine with different water contents.

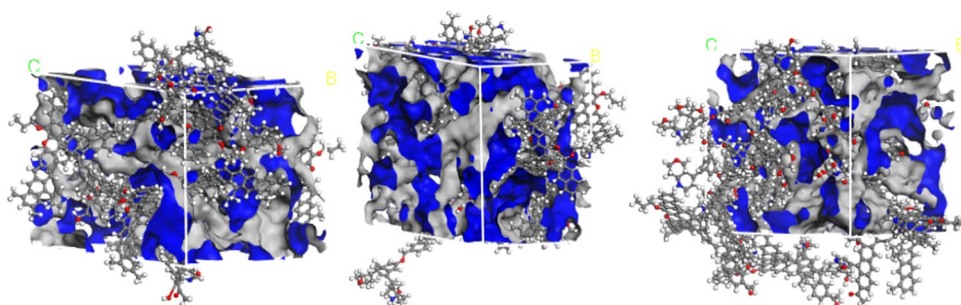


Figure 2. Ultracrystalline cell structure of Linglu mine coal with different water contents.

Setting	Parameter
Force field	Dreiding
Quality	Fine
Electrostatic	Atom based
van der Waals	Atom based
Cutoff distance	15.5 Å
Charges	QEq
Maximum iteration steps	20,000
Energy convergence values	0.0001 kcal/mol

Table 3. Simulation parameter settings.

step size was 1 fs, and the total simulation time was 500 ps, of which the first 60 ps were used to bring the system to equilibrium and the middle 60–100 ps to determine its diffusion properties.

Results and discussion

Influence of water content on CO₂, CH₄, and N₂ sorption and adsorption heat trends

Adsorption capacity

The sorption of CO₂, CH₄, and N₂ using the structural model of the Linglu mine coal was calculated at different temperatures (273.15, 283.15, 293.15, 303.15, and 313.15 K), pressures (0.1–10 MPa), and moisture contents (0%, 1.2%, 2.4%, and 3.6%), as shown in Fig. 1. The coal molecules were modeled with 0, 10, 20, and 30 water molecules.

The formula for calculating the water content³² is as follows:

$$W = \frac{M_{H_2O}}{M_{coal} + M_{H_2O}} \times 100\% \quad (1)$$

where $M_{\text{H}_2\text{O}}$ is the molecular weight of water, g/mol; M_{coal} is the molecular weight of coal, g/mol; and W is the water content, %.

As can be seen from Fig. 3, when the pressure in the system is from 0.1 to 1 MPa, the rising trend of the adsorption amount of CO_2 , CH_4 and N_2 rises rapidly with the increase of pressure, and the rising trend of the adsorption amount of the three kinds of gases is gradually smooth when the pressure is from 1 to 10 MPa, which indicates that the adsorption rate of the gases is more rapid in the low-pressure stage. The adsorption of the three gases decreases rapidly with increasing temperature. Clearly, increasing the pressure and decreasing the temperature were favorable to the adsorption of these gases. As shown in Fig. 3, the rise and fall trends of CO_2 , CH_4 , and N_2 adsorption by coal with different water contents were investigated at a pressure of 10 MPa and a temperature of 293.15 K as an example. A comparison of Fig. 3a–d shows that CO_2 adsorption decreases from 6.87 to 6.57 mmol/g, from 6.57 to 7.88 mmol/g, and from 7.88 to 4.23 mmol/g, respectively, when the water content in the system is increased from 0 to 1.2%, 2.4%, and 3.6%. Similarly, a comparison between Fig. 3e–l shows that the rise and fall trends of CH_4 and N_2 adsorption are the same as that of CO_2 adsorption. As shown in Fig. 4, the rise and fall trends of CO_2 , CH_4 , and N_2 adsorption in the system appears to be decreasing, then increasing, and finally decreasing. The reason for this phenomenon may be that the adsorption of coal on water molecules belongs to multilayer adsorption³³, and initially the water molecules are easy to form hydrogen bonding with the oxygen-containing functional groups in the coal molecules^{34,35}, but the hydrogen bonding belongs to the weak intermolecular interactions, and the interaction energies of the water molecules adsorbed on the hydroxyl groups are much larger than the interaction energies adsorbed on the other reactive groups³⁶. With the increase in the number of water molecules in coal, the oxygen-containing functional groups in the system will promote the competition between water molecules and CO_2 , CH_4 , and N_2 adsorption, resulting in a regional increase in the adsorption of the three gases, CO_2 , CH_4 , and N_2 ³⁷. Finally, after all the oxygenated functional groups in the coal were occupied, the excess water molecules began to adsorb on the pore surface of the coal in the form of free water, and they continuously condensed, eventually forming a water condensation film on the pore surface, which inhibited the sorption of CO_2 , CH_4 , and N_2 by the coal. Ultimately, the adsorption amount reduced.

Adsorption heat

Adsorption heat is one of the important parameters to characterize thermodynamics in order to respond to the thermic effect generated by the sorption process of water molecules on CO_2 , CH_4 , and N_2 . During the sorption process, the gas molecules move to the surface of the coal, where the speed of molecular motion is significantly reduced, thus releasing a large amount of heat. Table 4 shows the average sorption heat of CO_2 , CH_4 , and N_2

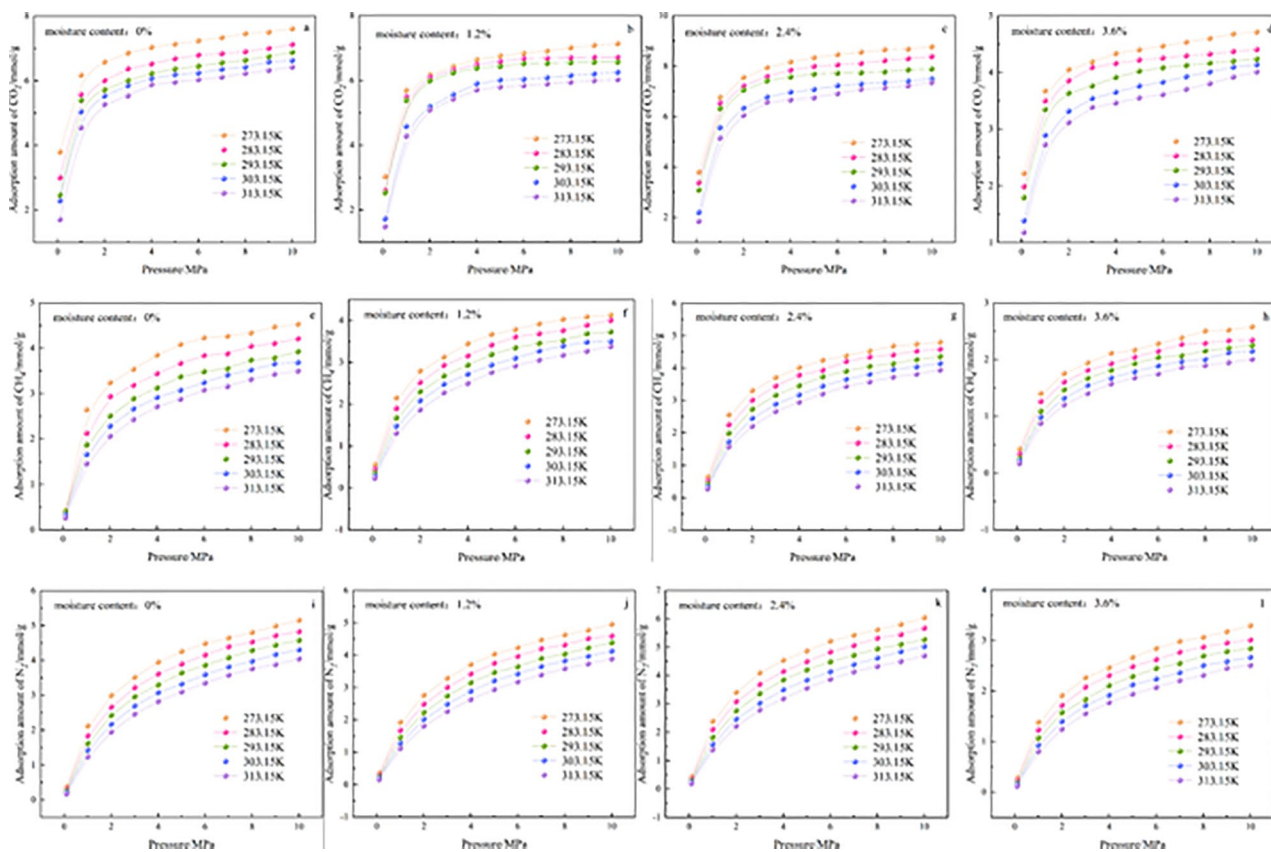


Figure 3. Isothermal sorption curves of CO_2 , CH_4 , and N_2 adsorbed by coal molecules with different water contents.

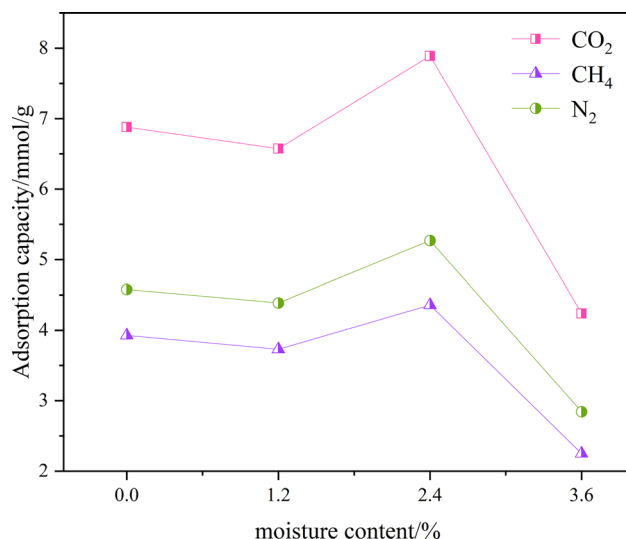


Figure 4. Rise and fall trends of CO₂, CH₄, and N₂ adsorption at a pressure of 10 MPa and a temperature of 293.15 K.

Moisture content/%	Gas	Average heat of adsorption/(kcal/mol)				
		273.15 K	283.15 K	293.15 K	303.15 K	313.15 K
0%	CO ₂	7.703	7.430	7.236	7.129	7.072
	CH ₄	4.552	4.495	4.443	4.419	4.388
	N ₂	3.755	3.740	3.730	3.713	3.701
1.2%	CO ₂	7.485	7.148	7.011	6.896	6.855
	CH ₄	4.394	4.376	4.354	4.339	4.322
	N ₂	3.686	3.678	3.668	3.664	3.655
2.4%	CO ₂	7.538	7.185	7.034	6.928	6.897
	CH ₄	4.400	4.385	4.370	4.343	4.329
	N ₂	3.739	3.726	3.711	3.698	3.688
3.6%	CO ₂	7.808	7.522	7.293	7.197	7.165
	CH ₄	4.819	4.803	4.792	4.785	4.772
	N ₂	4.038	4.030	4.024	4.019	4.012

Table 4. Average sorption heat of CO₂, CH₄, and N₂ at various temperatures and water content conditions.

adsorbed by coal molecules of various water contents at various temperatures and pressure ranging from 0.1 to 10 MPa.

As shown in Fig. 5, at a temperature of 273.15 K, as the water content in the system is increased from 0 to 1.2%, the average sorption heats of CO₂, CH₄, and N₂ decrease, respectively, from 7.70 to 7.48 kcal/mol, from 4.55 to 4.39 kcal/mol, and from 3.75 to 3.69 kcal/mol. When the water content in the system is increased from 1.2 to 2.4%, the average sorption heats of CO₂, CH₄, and N₂ increase from 7.48 to 7.54 kcal/mol, from 4.39 to 4.40 kcal/mol, and from 3.69 to 3.74 kcal/mol, respectively. When the water content is increased from 2.4 to 3.6%, the average sorption heats of CO₂, CH₄, and N₂ increase from 7.54 to 7.81 kcal/mol, from 4.40 to 4.82 kcal/mol, and from 3.74 to 4.04 kcal/mol, respectively.

Clearly, the average sorption heats of CO₂, CH₄, and N₂ showed a decreasing trend with increasing temperature. However, the average heat of adsorption showed an increasing trend with an increase in the water content in the system from 1.2 to 3.6%. From a thermodynamic viewpoint, this phenomenon can be attributed to increase in the density of the water molecules in the system, and their values gradually stabilized as the optimization process approached 500 ps, as shown in Fig. 6, in which the densities converged to 0.855, 0.873, and 0.948 g/cm³, respectively, for water contents of 1.2%, 2.4%, and 3.6%. Therefore, the trend in the average sorption heat was consistent with the trend in the density of the H₂O molecules in the system, indicating that the average sorption heat of the molecules in the Linglu mine coal with different water contents increases with the increase in the density of the system.

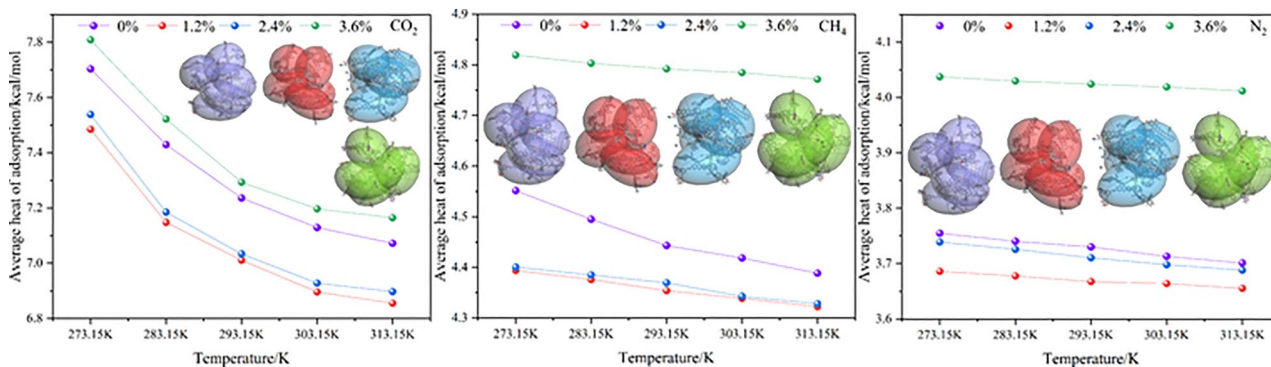


Figure 5. Trends in the average sorption heat of CO₂, CH₄, and N₂ at various temperatures and moisture contents.

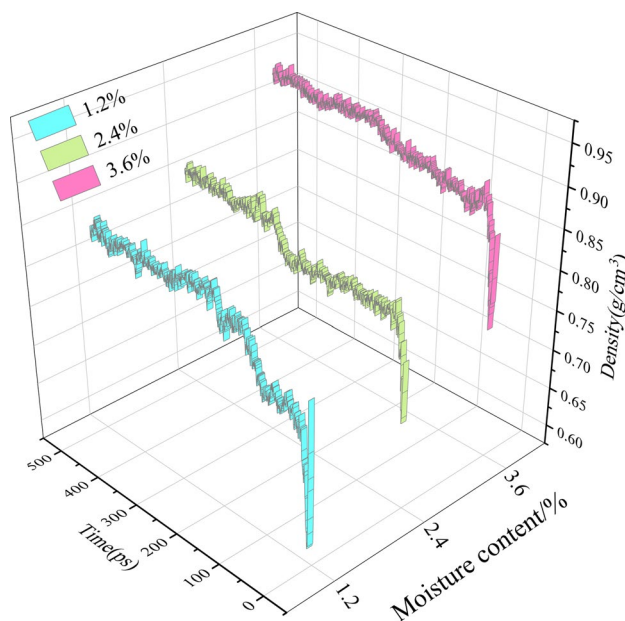


Figure 6. Density distribution of the coal molecules in the Linglu mine with different water contents.

Radial distribution function (RDF) and diffusive behavior (MSD)

Radial distribution function

The RDF is a physical quantity that characterizes the microstructural features of particles, and its physical meaning is the probability that other particles would appear at a distance r around an arbitrarily specified central particle, which can be interpreted as the ratio of the local density of the system to its mean bulk density. The radial distribution function $g(r)$ is given by Eq.³⁸:

$$g(r) = \frac{dN}{4\pi\rho r^2 dr} \quad (2)$$

where dN corresponds to the range r to $r + dr$:

$$dN = 4\pi r^2 \rho g(r) dr \quad (3)$$

where ρ is the density of the particle.

As shown in Fig. 7, with the addition of different amounts of water (1.2%, 2.4%, and 3.6%) to the system, the H₂O molecules showed the first peak at 0.975 Å, with the peaks being 1200.31, 638.13, and 371.65, respectively. A second peak occurred at 1.525 Å with peaks of 132.94, 73.45, and 41.78, respectively. From these two peaks, it can be seen that the H₂O molecules exhibited the highest peak when the water content in the system was 1.2%, followed by that when the water contents were 2.4% and 3.6%. The difference in the peaks indicates that, the fewer the H₂O molecules added to the molecular model of the Linglu mine coal (10–30 molecules), the tighter the arrangement of the H₂O molecules in the pores. The H₂O molecules showed a third peak at 2.875 Å with peaks of 10.07, 18.35, and 7.71, marking the formation of a layer of H₂O molecules with a layer spacing greater

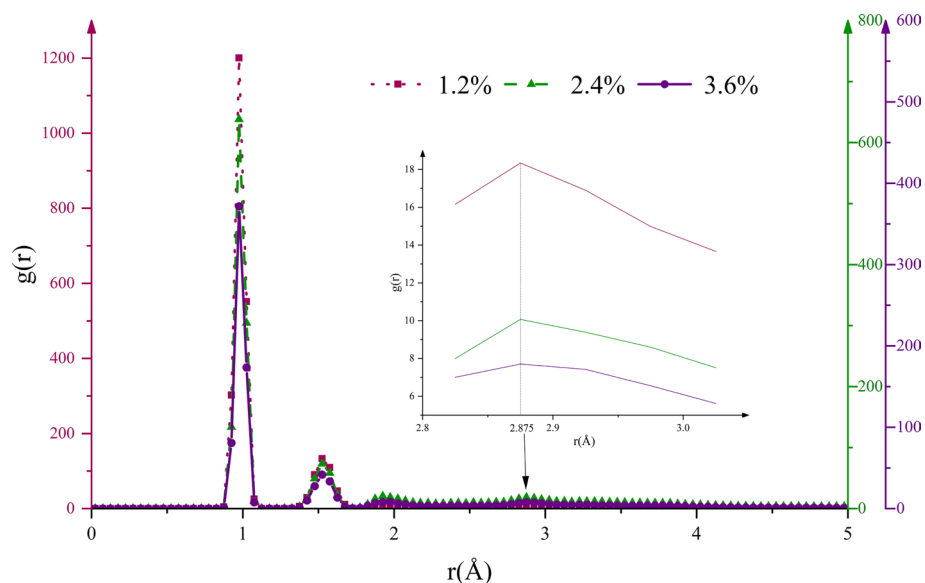


Figure 7. Radial distribution function of the molecules in Linglu mine coal with different water contents in the pores at a temperature of 293.15 K.

than the liquid–water layer spacing at 2.86 Å³⁹. When the water contents in the system were 1.2%, 2.4%, and 3.6%, the H₂O molecules competed for adsorption with CO₂, CH₄, and N₂ in the preliminary stage due to the lack of formation of the water molecule layer, resulting in an elevated adsorption of the three gases in the system. The sorption of CO₂, CH₄, and N₂ by the Linglu mine coal reduced in the later stage due to the formation of the H₂O molecular layer. This conclusion is consistent with that arrived at in Sect “Adsorption capacity”.

Diffusion coefficients

The diffusion behavior of a substance in a pore is proportional to the mean-square displacement of the center of mass of its molecules, and the corresponding diffusion coefficient is the rate of change in the mean-square displacement of all the molecules of the substance over a long duration⁴⁰, and the MSD is calculated using the equation:

$$MSD = \frac{1}{N} \sum_{i=1}^N [r_i(t) - r_i(0)]^2 \quad (4)$$

where N is the number of molecules; $r_i(0)$ is the initial site vector of the molecule; and $r_i(t)$ is the molecular site vector at time t .

The diffusion coefficient of a gas, Eq. 41, is given below:

$$D = \frac{1}{6N} \lim_{t \rightarrow \infty} \frac{d}{dt} \sum_{i=1}^N [r_i(t) - r_i(0)]^2 \quad (5)$$

$$D = \lim_{t \rightarrow \infty} \left(\frac{MSD}{6t} \right) = \frac{1}{6} k_{MSD} \quad (6)$$

where D is the diffusion coefficient of the gas; k_{MSD} is the slope of the MSD curve.

Diffusion coefficient is a physical quantity that describes the process of diffusion of a substance in space, and is the amount of substance per unit time, per unit area, that diffuses in the direction of lower concentration. Figure 8 shows the MSD versus time curves for CO₂, CH₄, and N₂ after water injection. It can be seen that the diffusion coefficient of N₂ in the system is obviously larger than that of CH₄ and CO₂, and the increase of water content did not inhibit the diffusion rate of N₂. The trend of the curves shows that water content has a more significant effect on the diffusion capacity of N₂, followed by CH₄ and CO₂.

The diffusion coefficients of CO₂, CH₄, and N₂ in coal molecules under the conditions of different water content are shown in Table 5. When the water content is 1.2%, the diffusion coefficients of CO₂, CH₄, and N₂ are 6.38×10^{-7} , 2.26×10^{-6} , and 7.47×10^{-6} cm²·s⁻¹, respectively; when the water content is 3.6%, the diffusion coefficients of CO₂, CH₄, and N₂ were 2.77×10^{-7} , 3.83×10^{-7} , and 3.53×10^{-6} cm²·s⁻¹, respectively. This is because with the increase of water content, the collision efficiency between the molecules increases, and the interaction force between them is strengthened, resulting in the inhibition of the diffusion of CO₂, CH₄, and N₂ in the pores, leading to a low diffusion coefficient.

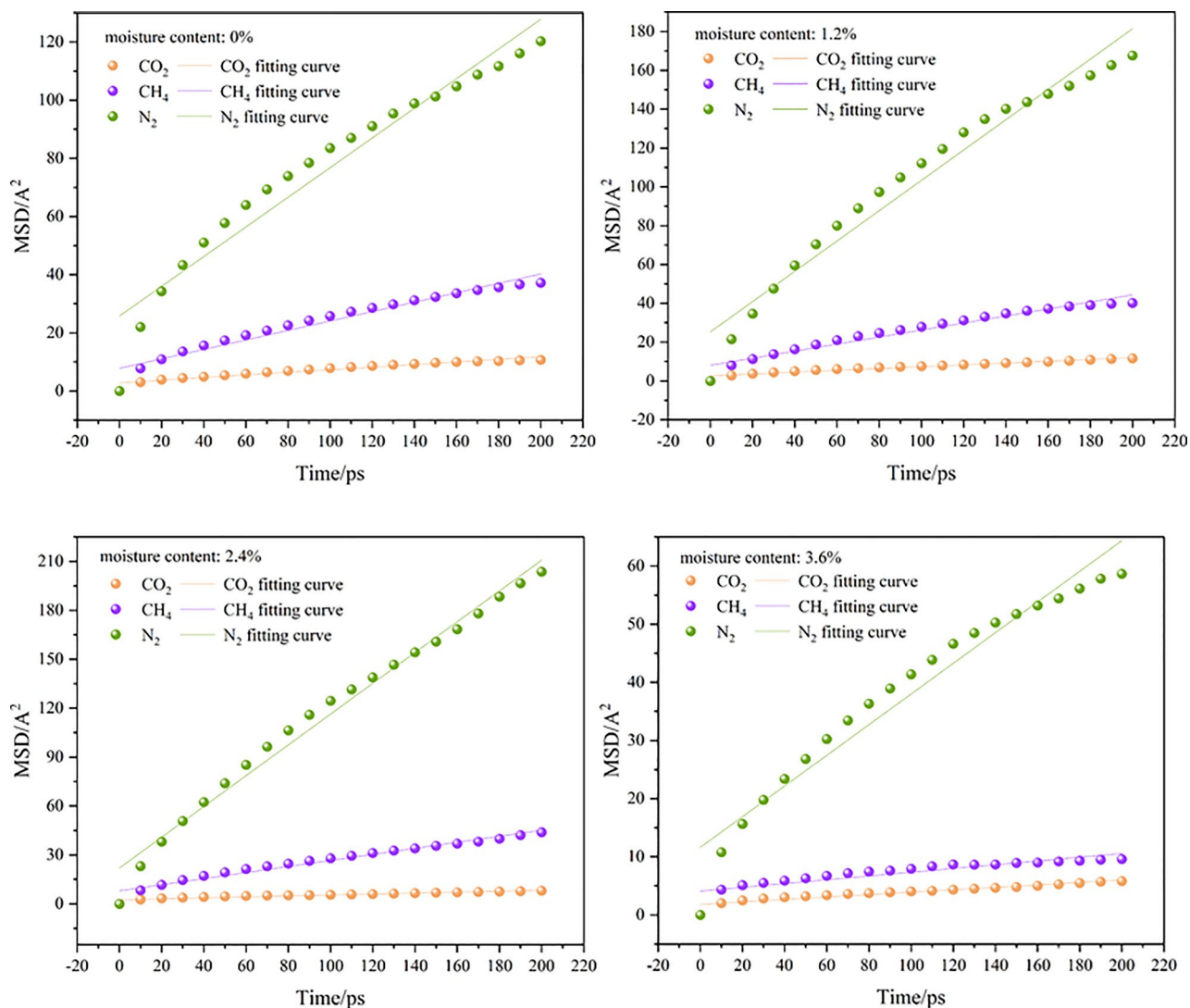


Figure 8. MSD vs. time for CO₂, CH₄, and N₂.

Moisture content	D/cm ² ·s ⁻¹		
	CO ₂	CH ₄	N ₂
0%	6.47×10^{-7}	2.30×10^{-6}	7.52×10^{-6}
1.2%	6.38×10^{-7}	2.26×10^{-6}	7.47×10^{-6}
2.4%	4.17×10^{-7}	2.08×10^{-6}	4.51×10^{-6}
3.6%	2.77×10^{-7}	3.83×10^{-7}	3.53×10^{-6}

Table 5. Diffusion coefficients of CO₂, CH₄ and N₂ in coal molecules.

Potential energy distribution

The potential energy distribution of CO₂, CH₄, and N₂ adsorbed by the coal molecules in the Linglu mine was simulated at a temperature of 293.15 K and a pressure of 10 MPa, as shown in Fig. 9. The effect of the water content in the coal molecules on the preferential adsorption potential of CO₂, CH₄, and N₂ was analyzed.

Figure 9 shows that the absolute value of the potential energy peak exhibits a trend of increasing and then decreasing in systems with water contents of 1.2%, 2.4%, and 3.6%. This is mainly because of the formation of ionic and covalent bonds between the adsorbed particles and atoms during the adsorption process, forming an ordered covering layer on the surface of molecules^{42,43}. When an adsorbed particle is close to the surface, it is subjected to an adsorption potential, and the adsorbed particle releases energy and adsorbs at the position where the potential energy of the molecule's surface has a minimum value. Interactions between its adsorbed atoms change the potential energy distribution on the surface. This is the main reason why the potential energy

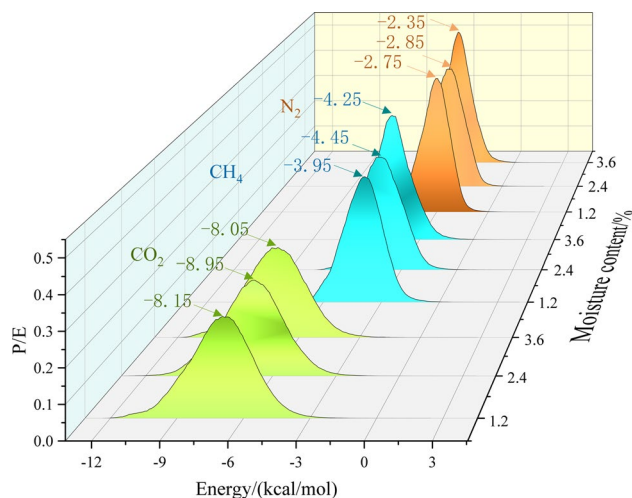


Figure 9. Potential energy distribution of gases adsorbed by coal with different water contents.

distribution graph shows a rise and then a fall. With the increase in the water content, the peak potential energies of the optimal adsorption sites of CO_2 , CH_4 , and N_2 in the system were compared, and the peak potential energies of CO_2 were -8.15 , -8.95 , and -8.05 kcal/mol, respectively, under the different water contents. The peak potential energies of CH_4 were -3.95 , -4.45 , and -4.25 kcal/mol, respectively. The peak potential energies of N_2 were -2.75 , -2.85 , and -2.35 kcal/mol, respectively. The sorption advantage of CO_2 was significantly greater than those of CH_4 and N_2 . Therefore, it can be concluded that the presence of water does not inhibit the CO_2 adsorption advantage.

Conclusions

- (1) With the increase in the water content from 0 to 3.6% in the system, with the adsorption amount of CO_2 being approximately twice as much as those of CH_4 and N_2 . This indicates that the presence of water had almost no effect on the sorption advantage of CO_2 .
- (2) The average sorption heat in the system was negatively correlated with the density of the water molecules, CO_2 emitted more heat during adsorption, resulting in its average heat of adsorption being significantly greater than those of CH_4 and N_2 .
- (3) The effect of water content on the diffusion ability of N_2 is more significant, followed by CH_4 and CO_2 . The diffusion coefficients of these three gases decreased gradually with the increase of water molecules. Based on the radial distribution function, the molecular layer spacing of the H_2O molecules (2.875 \AA) was greater than the liquid–water layer spacing of 2.86 \AA . Therefore, the adsorption of CO_2 , CH_4 , and N_2 was inhibited by the formation of the water molecule layer.
- (4) At the same temperature and pressure, and water contents of 1.2%, 2.4%, 3.6%, in terms of the sorption potential, the absolute values of the potential energy peaks of CO_2 , CH_4 , and N_2 increased and then decreased, with the same trend as its adsorption amount.

Data availability

All data supporting the findings of this study are available from the corresponding author Jiaying Lin upon request.

Received: 29 June 2024; Accepted: 31 July 2024

Published online: 06 August 2024

References

1. Busch, A. & Gensterblum, Y. CBM and CO_2 -ECBM related sorption processes in coal: A review. *Int. J. Coal Geol.* **87**, 49–71. <https://doi.org/10.1016/j.coal.2011.04.011> (2011).

2. Gao, Z. & Yang, W. Adsorption mechanism of water molecule on different rank coals molecular surface. *J. China Coal Soc.* **42**, 753–759. <https://doi.org/10.13225/j.cnki.jccs.2016.0642> (2017).
3. Nie, B., He, X., Wang, E. & Zhang, L. Micro-mechanism of coal adsorbing water. *J. China Univ. Min. Technol.* **33**, 17–21 (2004).
4. Sang, S., Zhu, Y., Zhang, J., Zhang, X. & Zhang, S. Experimental study on the effect of liquid water on methane adsorption by coal: A case study of coal reservoirs in the southern Qinshui Basin. *Chin. Sci. Bull.* **50**, 79–85 (2005).
5. Zhang, S. & Sang, S. Influence mechanism of liquid water on methane absorption of coals with different ranks. *Acta Geol. Sin.* **82**, 1350–1354 (2008).
6. Zhiguo, X. & Leiting, M. Experimental study on the inhibitory effect of the gas desorption in the coal seam water-infusion. *J. Saf. Environ.* **15**, 55–59. <https://doi.org/10.13637/j.issn.1009-6094.2015.02.012> (2015).
7. Feng, Y. & Dong, H. Estimation of coal seam gas pressure based on gas desorption characteristics of coal with different moisture contents. *Saf. Coal Mines* **54**, 8–14. <https://doi.org/10.13347/j.cnki.mkaq.2023.09.002> (2023).
8. Liu, X., Zhang, Y., Zhang, X., Wang, J. & Zhou, C. Study on the effect and mechanism of original moisture on coal spontaneous combustion. *J. Taiyuan Univ. Technol.* **52**, 350–359 (2021).
9. Nie, B. *et al.* Sorption characteristics of methane among various rank coals: Impact of moisture. *Adsorption* **22**, 315–325. <https://doi.org/10.1007/s10450-016-9778-9> (2016).
10. Tang, X. Simulation of CO₂ and O₂ adsorption in bituminous coals with different moisture contents. *Inn. Mong. Coal Econ.* <https://doi.org/10.13487/j.cnki.imce.024146> (2023).
11. Zhu, H. *et al.* Thermodynamic characteristics of methane adsorption about coking coal molecular with different sulfur components: Considering the influence of moisture contents. *J. Nat. Gas Sci. Eng.* <https://doi.org/10.1016/j.jngse.2021.104053> (2021).
12. Kang, N., Chen, X., Yang, H., Zhao, S. & Qi, L. Effect of different placement sequences of water on the methane adsorption properties of coal. *ACS Omega* **8**, 6689–6698. <https://doi.org/10.1021/acsomega.2c07283> (2023).
13. Li, Y., Yang, Z. & Li, X. Molecular simulation study on the effect of coal rank and moisture on CO₂/CH₄ competitive adsorption. *Energy Fuels* **33**, 9087–9098. <https://doi.org/10.1021/acs.energyfuels.9b01805> (2019).
14. Li, Z., Bai, Y., Yu, H., Hu, H. & Wang, Y. Molecular simulation of thermodynamic properties of CH₄ and CO₂ adsorption under different moisture content and pore size conditions. *Fuel* <https://doi.org/10.1016/j.fuel.2023.127833> (2023).
15. Gao, D. & Xu, X. Molecular simulation on the influence of FeS₂ on anthracite adsorption of CH₄ and O₂. *J. Saudi Chem. Soc.* <https://doi.org/10.1016/j.jscs.2024.101823> (2024).
16. Hong, L., Lin, J., Gao, D. & Zheng, D. Molecular modeling of CO₂ affecting competitive adsorption within anthracite coal. *Sci. Rep.* <https://doi.org/10.1038/s41598-024-58483-z> (2024).
17. Zhang, X. *et al.* Thermodynamic characteristics of methane adsorption on coals from China with selected metamorphism degrees: Considering the influence of temperature, moisture content, and in situ modification. *Fuel* <https://doi.org/10.1016/j.fuel.2023.127771> (2023).
18. Gao, D. & Song, Z. Study on gas adsorption and desorption characteristics on water injection coal. *J. Saudi Chem. Soc.* <https://doi.org/10.1016/j.jscs.2023.101645> (2023).
19. Zhang, G.-H., Liu, X.-X., Bi, Y.-W. & Pu, W.-L. Experimental study of water effects on gas desorption during high-pressure water injection. *J. Coal Sci. Eng.* **17**, 408–413. <https://doi.org/10.1007/s12404-011-0409-5> (2011).
20. Li, Y. *et al.* Characterizing water vapor adsorption on coal by nuclear magnetic resonance: Influence of coal pore structure and surface properties. *Energy* <https://doi.org/10.1016/j.energy.2023.128420> (2023).
21. Wang, F., Yao, Y., Wen, Z., Sun, Q. & Yuan, X. Effect of water occurrences on methane adsorption capacity of coal: A comparison between bituminous coal and anthracite coal. *Fuel* <https://doi.org/10.1016/j.fuel.2020.117102> (2020).
22. Xing, Y., Xiao, X., Zhou, Q., Liu, W. & Zhao, Y. Influence of water on the methane adsorption capacity of organic-rich shales and its controlling factors: A review. *Energies* <https://doi.org/10.3390/en16083305> (2023).
23. Han, W., Li, A., Memon, A. & Ma, M. Synergetic effect of water, temperature, and pressure on methane adsorption in shale gas reservoirs. *ACS Omega* **6**, 2215–2229. <https://doi.org/10.1021/acsomega.0c05490> (2021).
24. Zhang, Q., Liu, X., Nie, B., Wu, W. & Wang, R. Methane sorption behavior on tectonic coal under the influence of moisture. *Fuel* <https://doi.org/10.1016/j.fuel.2022.125150> (2022).
25. Guo, H., Cheng, Y., Wang, L., Lu, S. & Jin, K. Experimental study on the effect of moisture on low-rank coal adsorption characteristics. *J. Nat. Gas Sci. Eng.* **24**, 245–251. <https://doi.org/10.1016/j.jngse.2015.03.037> (2015).
26. Chattaraj, S., Mohanty, D., Kumar, T. & Halder, G. Thermodynamics, kinetics and modeling of sorption behaviour of coalbed methane—A review. *J. Unconv. Oil Gas Resour.* **16**, 14–33. <https://doi.org/10.1016/j.juogr.2016.09.001> (2016).
27. Men'shchikov, I. E., Shkolin, A. V., Fomkin, A. A. & Khozina, E. V. Thermodynamics of methane adsorption on carbon adsorbent prepared from mineral coal. *Adsorption* **27**, 1095–1107 (2021).
28. Gensterblum, Y., Merkel, A., Busch, A. & Krooss, B. M. High-pressure CH₄ and CO₂ sorption isotherms as a function of coal maturity and the influence of moisture. *Int. J. Coal Geol.* **118**, 45–57. <https://doi.org/10.1016/j.coal.2013.07.024> (2013).
29. Muangthong-on, T., Wannapeera, J., Ohgaki, H. & Miura, K. TG-DSC study to measure heat of desorption of water during the thermal drying of coal and to examine the role of adsorption of water vapor for examining spontaneous heating of coal over 100 °C. *Energy Fuels* **31**, 10691–10698. <https://doi.org/10.1021/acs.energyfuels.7b01836> (2017).
30. Tan, B. *et al.* Molecular simulation for physisorption characteristics of O₂ in low-rank coals. *Energy* <https://doi.org/10.1016/j.energy.2021.122538> (2022).
31. Wang, Z., Li, Y., Wang, Z. & Zhou, L. Factors influencing the methane adsorption capacity of coal and adsorption heat variations. *Energy Fuels* **37**, 13080–13092. <https://doi.org/10.1021/acs.energyfuels.3c02339> (2023).
32. Liwei, C., Dongjie, W., Le, B., Yuan, L. & Xiaohua, L. Study on the influence of coal seam water content on the effect of CO₂ isobaric diffusion displacing CH₄. *Coal Sci. Technol.* <https://doi.org/10.12438/cst.2024-0061> (2024).
33. Wang, C. *et al.* Adsorption of water on carbon materials: The formation of “water bridge” and its effect on water adsorption. *Colloids Surf. A Physicochem. Eng. Asp.* <https://doi.org/10.1016/j.colsurfa.2021.127719> (2021).
34. Zhiqiang, X., Xiangyang, L., Yanan, T., Dinghua, L. & Guanlin, R. Quantum chemical calculation of the interaction between lignite and water molecules. *J. China Univ. Min. Technol.* **51**, 554–561. <https://doi.org/10.13247/j.cnki.jcmt.001411> (2022).
35. Wu, J. *et al.* Moisture removal mechanism of low-rank coal by hydrothermal dewatering: Physicochemical property analysis and DFT calculation. *Fuel* **187**, 242–249 (2017).
36. Zhengyang, G., Shaokun, L., Jinda, L., Pengfei, Y. & Chuanmin, C. Micro-mechanism of water molecule adsorption on lignite surfaces. *J. Chin. Soc. Power Eng.* **36**, 258–264 (2016).
37. Jianhua, X. & Lei, L. Study on influence of coal surface functional groups on methane and carbon dioxide adsorption properties. *Coal Sci. Technol.* **49**, 145–151. <https://doi.org/10.13199/j.cnki.cst.2021.06.017> (2021).
38. Xu, W. *et al.* Molecular dynamic investigations on the adhesion behaviors of asphalt mastic-aggregate interface. *Materials* <https://doi.org/10.3390/ma13225061> (2020).
39. Jianhua, X., Fangui, Z., Huzhen, L., Bin, L. & Xiaoxia, S. Molecular simulation of the CH₄/CO₂/H₂O adsorption onto the molecular structure of coal. *Sci. China Earth Sci.* **44**, 1418–1428 (2014).
40. You, X. *et al.* Molecular dynamics simulations and contact angle of surfactant at the coal–water interface. *Mol. Simul.* **44**, 722–727. <https://doi.org/10.1080/08927022.2018.1441530> (2018).
41. Xia, Y., Yang, Z., Zhang, R., Xing, Y. & Gui, X. Enhancement of the surface hydrophobicity of low-rank coal by adsorbing DTAB: An experimental and molecular dynamics simulation study. *Fuel* **239**, 145–152. <https://doi.org/10.1016/j.fuel.2018.10.156> (2019).

42. Yunfei, Z. & Yan, L. Study of graphene wear based on coupled interfacial bonding effects. *J. At. Mol. Phys.* <https://doi.org/10.19855/j.1000-0364.2025.062003> (2025).
43. Shaohong, Z., Haikuan, Y., Kai, W., Jiamin, L. & Jide, L. Influence of diamine structural units on thermosetting polymer with dynamic covalent bonds. *New Chem. Mat.* <https://doi.org/10.19817/j.cnki.issn1006-3536.2024.10.033> (2024).

Acknowledgements

The authors would like to thank all the reviewers who participated in the review, as well as MJEditor (www.mjeditor.com) for providing English editing services during the preparation of this manuscript.

Author contributions

The data were analyzed by H.L. and G. D., Z. D., W. W. analyzed the images, and L.J. wrote the manuscript.

Funding

This work is supported by the National Natural Science Foundation of China (Grant No.52074147), Liaoning Natural Science Foundation of China (Grant No. LJKQZ20222334) and Liaoning Province Education Administration (Grant No. LJ2017FBL001).

Competing interests

The authors declare no competing interests.

Additional information

Correspondence and requests for materials should be addressed to J.L.

Reprints and permissions information is available at www.nature.com/reprints.

Publisher's note Springer Nature remains neutral with regard to jurisdictional claims in published maps and institutional affiliations.

Open Access This article is licensed under a Creative Commons Attribution-NonCommercial-NoDerivatives 4.0 International License, which permits any non-commercial use, sharing, distribution and reproduction in any medium or format, as long as you give appropriate credit to the original author(s) and the source, provide a link to the Creative Commons licence, and indicate if you modified the licensed material. You do not have permission under this licence to share adapted material derived from this article or parts of it. The images or other third party material in this article are included in the article's Creative Commons licence, unless indicated otherwise in a credit line to the material. If material is not included in the article's Creative Commons licence and your intended use is not permitted by statutory regulation or exceeds the permitted use, you will need to obtain permission directly from the copyright holder. To view a copy of this licence, visit <http://creativecommons.org/licenses/by-nc-nd/4.0/>.

© The Author(s) 2024